In vivo evaluation of a biomimetic apatite coating grown on titanium surfaces

Deepta Vani Vasudev,[1] John L. Ricci,[2] Christopher Sabatino,[1] Panjian Li,[3] J. Russell Parsons[1]
[1]*UMDNJ-New Jersey Medical School, Department of Orthopaedics, 185 South Orange Avenue, MSB G-574, Newark, New Jersey 07103*
[2]*New York University College of Dentistry, Department of Biomaterials & Biomimetics, 345 E. 24th Street 816A, New York, New York 10010*
[3]*DePuy Orthopaedics Inc., 700 Orthopaedic Drive, Warsaw, Indiana 46581*

Received 15 December 2003; accepted 3 February 2004
Published online 3 May 2004 in Wiley InterScience (www.interscience.wiley.com). DOI: 10.1002/jbm.a.30028

Abstract: Osteoconductive mineral coatings represent an established technology for enhancing the integration of orthopedic implants with living bone. However, current coatings have limitations related to fabrication methods, attachment strength to metal substrates, and in vivo performance. Low temperature biomimetic growth is a coating technique wherein the device to be coated is immersed in a meta-stable saturated solution of the coating constituents and growth of the coating is then allowed to proceed on the surface of the device. This study focused on the *in vivo* evaluation of a biomimetic apatite coating fabricated under these conditions. The experiment was designed to specifically test the amount of bone ingrowth into the coated channels versus the uncoated channels of an established bone chamber system, with emphasis placed on the amount of bone present on the coupon surface. Three types of measurements were taken on each channel: linear ingrowth %, area ingrowth %, and continuous bone apposition %. The experiments demonstrated that under controlled conditions, the apatite coating appears to resorb in 8 weeks and did stimulate early osseointegration with the metal surface with a reduction in fibrous tissue encapsulation. This coating may, therefore, be useful in facilitating early bone ingrowth into porous surfaces without the potential for coating debris, macrophage infiltration, fibrous tissue encapsulation, and eventual coating failure as may occur with current plasma-sprayed hydroxapatite coating techniques. © 2004 Wiley Periodicals, Inc. J Biomed Mater Res 69A: 629–636, 2004

Key words: hydroxyapatite; solution deposition fabrication method; bone-chamber model; orthopedic coatings; biomaterials

INTRODUCTION

Total joint replacement is currently the most common and successful elective orthopedic surgical procedure. Annually it is estimated that in the United States alone over 400,000 total joint replacements (TJR) are surgically implanted.[1] Worldwide the total annual number of joint replacements is approaching 700,000.[1,2] Of the joint replacements performed in the United States, approximately 60% are cemented in place with polymethyl methacrylate (PMMA) bone cement.[3–5] With modern implants, surgical procedures, and cement techniques, PMMA stabilized joint replacements are considered the "gold standard" with survival rates in excess of 10 years.[3–6] Long-term data for cemented joints, however, do show failure rates of up to 30% due to osteolysis at the bone-implant interface.[7–9]

The remaining approximately 40% of TJR utilize "uncemented" components or hybrid components (one component cemented). These uncemented implants rely on host bone ingrowth into a porous, textured surface for stabilization. There are a number of commercially available porous/textured surfaces for bone ingrowth stabilization of TJR, including: porous sintered metal beads and wires, and various post fabrication texturing techniques.[10–14] Generally, these uncemented implants have proven quite successful, and are often used in younger patients; however, concern still remains whether survival rates are currently equivalent to the "gold standard" or actually better.[10-17] What is known, however, is that bone ingrowth into porous surfaces is variable and seldom, if ever, complete. Animal studies, as well as human implant retrievals, reveal that at best only about 40% of the available surface porosity is actually filled with bone.[17,18] Conse-

Correspondence to: J. Russell Parsons; e-mail: parsonjr@umdnj.edu

quently, research over the past decade has concentrated on methodologies for encouraging faster and more robust bone ingrowth into porous coated implants.

Much of this research has focused on the development and use of new bioactive ceramic coating techniques, especially with hydroxyapatite (HA).[19] A coating of calcium phosphate ceramic (i.e., plasma-sprayed hydroxyapatite on a porous ingrowth implant surface) encourages rapid osteoconduction from adjacent bone and allows for direct chemical bonding to newly formed bone shortly after implantation.[20–24] The use of such bioactive coatings is thought to provide more rapid patient recovery, improved early range of motion, and decreased pain in short-term studies.[21–23] Most stable bioactive ceramic coatings on the market today are deposited onto porous implant surfaces using a plasma-spraying technique. Such a technique is mainly a line-of-sight methodology and, therefore, does not adequately cover the complex surfaces of an implant such as deep grooves or surface porosities.[25–29] Furthermore, plasma spraying is a high temperature process that inevitably causes some decomposition of HA leading to a mixture of several calcium phosphate phases including HA as the end product.[25,30] Despite the presence of multiple phases, currently utilized stable plasma sprayed HA coatings show little evidence of resorption up to 9 months postoperatively. Consequently, these coatings are thought to be susceptible to long-term failure at the coating/implant interface.[32] Such a coating failure could produce HA debris, which, in turn, could result in osteoclast activation, bone loss, and aseptic loosening.[20,31,33]

A more complete three-dimensional, low-temperature deposition technique may alleviate these problems. That is to say, a less stable bone-mineral-like coating could initially encourage rapid bone ingrowth, but would resorb in the short term, eliminating long-term interface failure and the consequences of ceramic debris production. Low-temperature biomimetic growth allows the device to be immersed in a metastable saturated solution of the coating constituents and the growth of the coating is then allowed to proceed on the implant surface. This results in three-dimensional uniform coverage of all areas of the implant, which improves the surface area of the coating exposed to ingrowing host bone. This may also increase bone ingrowth volume and, consequently, the fixation between implant and newly formed bone. Biomimetic deposition also differs from plasma spraying techniques in that it is a relatively low-temperature process. This allows the formulation of a low-density, biodegradable, thin coating on a surface.[34] The current study focuses on the in vivo evaluation of a biomimetic apatite coating formed using solution deposition techniques. The ability of this coating to promote bone ingrowth and apposition to the implant surface was assessed *in vivo* in an established canine bone chamber model.[35,36]

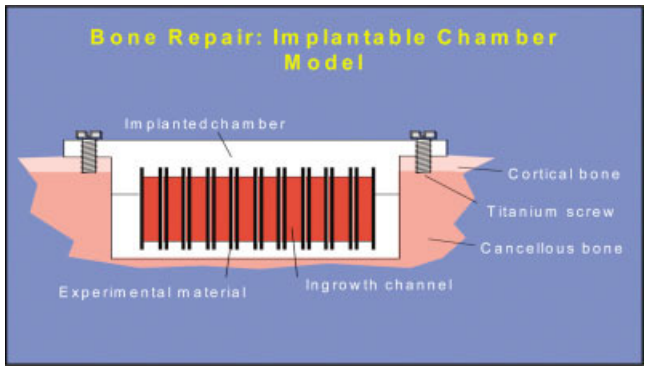

Figure 1. Schematic of bone chamber showing placement of 9 titanium coupons within the polyethylene shell. [Color figure can be viewed in the online issue, which is available at www.interscience.wiley.com.]

MATERIALS AND METHODS

Sixteen chambers were implanted into the lateral metaphysis of the distal femur of 8 skeletally mature, large coonhound dogs. Each animal received 2 chambers, one in each femur. Two animals were sacrificed at 6 weeks, 4 at 8 weeks, and 2 at 12 weeks. The femurs were harvested and processed for high-resolution X ray, histology, and backscattered electron imaging (BEI) analysis. X-ray and BEI images served to verify histomorphometric data. Bone linear ingrowth, area ingrowth, and continuous apposition percentages were then calculated for all images using the BIOQUANT (version 3.50.6) image analysis system. NIH guidelines for the care and use of laboratory animals (NIH Publication 85-23 Rev. 1985) have been observed.

Bone chamber characteristics

Five titanium alloy coupons (measuring 7 × 8 mm) were coated with the biomimetic apatite coating and placed consecutively in a pre-fabricated polyethylene shell (see Fig. 1). This bone chamber system has been used previously to test various materials *in vivo* for a side-by-side comparison.[35,36] Four other non-coated titanium coupons were placed at the other end of the chamber, to give a total of 9 coupons per bone chamber. All samples were oriented such that the 4 uncoated coupons sat on the side of the chamber designated by a notch. Each pair of coupons formed the two opposite walls of a narrow channel 1 mm wide. Each coupon had 5 × 8 mm of its surface exposed to the channel, making 40 mm^2 of surface area exposed to the channel per coupon. Therefore, a volume of 1 × 5 × 8 mm (or 40 mm^3) was available for tissue ingrowth between the coupons. Each channel was open at both ends to allow for tissue ingrowth, with each opening measuring 1 × 5 × 8 mm. The position of the control

(uncoated channels) sites was randomized by alternating the control side of the chamber from the proximal area of femur to the distal area of the femur.

Growth of biomimetic apatite layer

A dense, substantially pure ceramic coating with a crystal size of <1 μm was fabricated at DePuy Orthopaedics Inc. using the method described below.[37] The aqueous solution used in this study for growing biomimetic apatite coatings includes all major inorganic ions present in the body, namely Na^+, K^+, Mg^{2+}, Ca^{2+}, Cl^-, HPO_4^{2-}, HCO_3^-, and SO_4^2. The solution was prepared by dissolving $CaCl_2$, NaCl, KCl, K_2HPO_4, $MgCl_2$, $NaSO_4$, and $NaHCO_3$ in de-ionized H_2O, with the concentrations of $CaCl_2$, NaCl, KCl, $NaHCO_3$, $MgCl_2$, and $NaSO_4$ being at their corresponding levels in human blood plasma. The concentrations of Ca^{2+} and HPO_4^{2-} in the coating source solution range from 2.5 to 10 mM and from 1.0 to 6 mM, respectively. The pH of the as-prepared coating source solution was adjusted to neutral pH using tris(hydroxymethyl)aminomethane-hydrochloric acid. The Ti6Al4V coupons were fully immersed in the solution in a glass reactor at a temperature of 45°C. The pH of the solution spontaneously began increasing due to the release of HCO_3^- in the form of CO_2 into the above atmosphere. With the pH of the solution elevating, the coating began to form on the titanium surface. The coupons remained immersed in the solution for 4 days. Mineral coatings fabricated by this method were characterized by an absence of macropores and micropores and a small crystal size (<1 μm). The coating is similar to bone mineral in composition (as seen by scanning electron microscopy, thin-film X-ray diffractometer, diffuse reflectance Fourier transform infrared spectroscopy, and atomic absorption spectrophotometry).[34]

High resolution X-ray imaging

Each chamber was removed from the femur of each animal with approximately 2 mm of surrounding bone on either side of the openings of the channels. Soft tissue and overgrown bone were then removed from the top and bottom surface of the chamber in order to make the polyethylene shell visible on both ends. High-resolution X-ray imaging (Hewlett-Packard Faxitron X-ray imaging) of the implants were then taken (setting: 45 kV for 1 min) to visualize the bone ingrowth in the channels.

Histological processing

All specimens were then fixed in 70% ethanol for 3–6 days and processed for embedding in polymethylmethacrylate (PMMA). Undecalcified specimens embedded in PMMA were sectioned using a diamond wafering blade in a plane parallel to the tissue-coupon interface and slightly off center. The first section was saved for BEI analysis. Two additional slices, each 500 μm thick, were cut, ground, polished, and mounted onto acrylic slides. The slides were further ground to 200 μm and polished to achieve a final thickness of 150 μm. All slides were then stained using a Stevenel's Blue and Van Gieson's picrofucsin staining protocol, where bone stained red and nonmineralized soft tissues stained blue-green. Slides were then properly labeled with their ID and orientation and stored until analysis.

BEI analysis

Each specimen stored for BEI was polished and vapor deposited with a thin layer (approximately 60 nm) of carbon. These samples were analyzed using a Hitachi S2500 scanning electron microscope equipped with a GW Electronics backscattered electron imaging system. Metal was shown as bright white, bone was various shades of gray, and soft tissue was black.[36,38,39] This technique allowed for analysis of bone microstructure and the bone/implant interface of undisturbed, undecalcified samples, and was used to image all samples macroscopically. Since the system does not give low-magnification images, 8–10 frames were captured per sample and then formulated into a montage using Photoshop® (Microsoft, Inc.) software. The resulting image was saved and stored for Bioquant analysis. Further special emphasis was placed on the metal/bone interface. Representative samples for each time period were imaged under high magnification to capture the metal/bone interface for a coated coupon and an uncoated coupon. The coated coupons were also examined for the presence or absence of coating.

Histomorphometric analysis

For each channel, all histological, Faxitron, and BEI images were analyzed for percent bone linear ingrowth per channel, percent bone area ingrowth per channel, and percent continuous bone apposition to the control or experimental surface. All measurements used a Nikon Microphot-FX light microscope equipped with an Optronix digital video camera system and BioQuant (version 3.50.6) software.

Linear ingrowth measurements

As mentioned previously, each channel was lined on either side by control titanium coupons or experimental apatite-coated coupons. At 4× magnification, the length of each channel was measured end-to-end, then the furthest extent of bone penetration from each open end of the channel was measured. Each individual measurement was added together and divided by the total length of the channel. A measurement of 100% represented full bone penetration

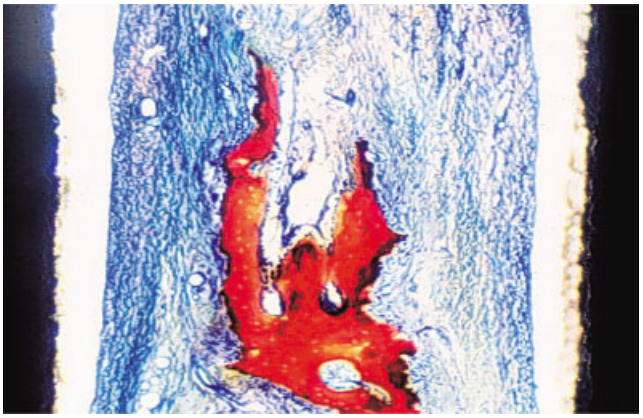

Figure 2. Histological slide of an uncoated channel at 6 weeks showing the extent of fibrous tissue encapsulation of the bone; notice the greater degree of fibrous tissue thickness in between bone and the metal in uncoated channels than in coated channels. [Color figure can be viewed in the online issue, which is available at www.interscience.wiley.com.]

from one end to the other end of the channel. Faxitron images and histological slides were used for these measurements and compared to one another.

Area ingrowth measurements

Each channel was selected as the region of interest to work with one at a time. Bone within the channel was selected and measured for its total area. The bone area was then normalized to the total area of the channel to give the percent area ingrowth. All measurements were conducted at 5× magnification. Histological slides and BEI images were used for these measurements and compared to one another.

Continuous bone apposition measurements

At 54× magnification, the total length of each coupon lining the channel was measured. Beginning with the left side, the coupon surface/bone interface was scanned for areas with direct bone contact. Direct bone contact was defined as any areas where there is no soft tissue between bone and metal, and where there is less than 10 μm separating bone from metal. The latter definition was added to remedy the separation that is evident from shrinkage artifact from preparing the slides. Areas of coupon surface with direct bone contact were measured and combined, and the resulting number was divided by the total length of the coupon surface. The same procedure was carried out for the right side of the channel, and a resulting average bone apposition was taken for each channel. For each chamber, 2 histological slides were used for these measurements.

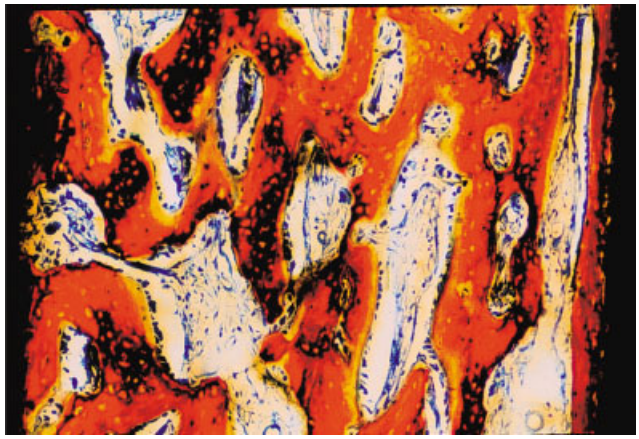

Figure 3. Histological slide of a coated channel at 6 weeks showing direct bone apposition to the metal surface and excessive bone remodeling; notice on left side of channel, an osteoclast is interspersed in between bone matrix and is degrading bone/coating at the interface. [Color figure can be viewed in the online issue, which is available at www.interscience.wiley.com.]

Statistics

All data was analyzed using SPSS 9.0 statistical software as a general linear model repeated measures experiment with dog ID as the only between-subject factor, with treatment, laterality, channels, and replicas as within-subject factors. Of the 8 channels that were formed by the coupons, the first 3 coated channels and the last 3 uncoated channels were used for analysis.

RESULTS

The bone and soft tissue response to the apatite-coated and uncoated titanium samples was easily vi-

Figure 4. Histological slide of a coated channel at 8 weeks showing the direct bone apposition to the metallic surface and the more remodeled mature bone matrix with a lesser degree of osteoblasts and osteoclasts than 6-week channels. [Color figure can be viewed in the online issue, which is available at www.interscience.wiley.com.]

TABLE I
Summary of Bone Linear Ingrowth Data From Histological Slides[a]

	Avg Coated Ingrowth		Avg Uncoated Ingrowth			
Study Group	%	SE	%	SE	*p* Value	Sample Size, n
6 week	75.85	10.22	58.85	5.52	0.065	30
8 week	80.48	8.34	55.07	4.51		
12 week	96.90	6.18	48.42	15.54	0.264	12

[a]Sample size includes repeated measures experiments done on a total of 6 channels per animal. SE, standard error.

sualized through all analytic modalities. At 6 weeks, the uncoated samples contained immature fibrous tissue, while the 8- and 12-week uncoated samples contained well-oriented fibrous tissue rich with fibroblasts. The fibrous tissue layer was continuous with an occasional projection of trabeculae through the fibrous interface layer (Fig. 2). In contrast, the apatite-coated samples had channels with far less fibrous tissue encapsulation than uncoated samples. They also contained a direct bone/implant interaction throughout a much greater portion of the channel length. Focal areas of osteoclastic activity interspersed between the attached bone and metal coupon were observed, with osteoclasts acting mainly on the deposited apatite layer (Figs. 3, 4). The histomorphometric linear ingrowth percentages were not statistically significant between the two treatments in both study groups, but were trending towards significance ($p = 0.065$) (see Table I). However, when Faxitron images were analyzed for linear ingrowth, significance was found between the two treatments in the 6- and 8-week study groups ($p = 0.013$) (see Table II). Significance was also found for histomorphometric area ingrowth (Table III) and BEI images (Table IV), as well as histomorphometric apposition percentages (Table V) between treatments in both study groups ($p < 0.05$).

DISCUSSION

Statistical analysis

Previous publications using a bone chamber model analyzed the data using a basic paired t-test.[35,36] However, since all channels within each chamber are linked by both location and animal, this method introduces a large amount of variability into the results, which leads to a large standard deviation. Due to this linkage between channels and chambers (two chambers are implanted into one animal), a paired t-test may not be the optimal analysis method to employ. This project employed a repeated measures experiment with dog ID as the only between-subject factor, with treatment, laterality, channels, and replicas as within-subject factors. After accumulating all data, it was found that 6- and 8-week specimens contained similar bone ingrowth patterns, so the two study groups were collapsed together during the statistical analysis. This decision was justified by the absence of a time by treatment interaction in the subsequent analysis. Also, initial analysis showed no treatment by laterality, treatment by channel, and treatment by replica correlation, so all within-subject factors were collapsed together to form one main within-subject factor; namely, treatment.

Linear ingrowth

The first phase of evaluation was performed by quantifying the extent of linear ingrowth into each coated and uncoated channel of each chamber. Histology slides display a two-dimensional view of each channel, and, therefore, may not contain the plane with the maximum extent of linear ingrowth. However, since all chambers were sectioned at the same location, the average relative difference between coated and uncoated channels should be representative. Also, faxitron images capture the greatest extent of bone ingrowth through the depth of each channel.

TABLE II
Summary of Bone Linear Ingrowth Data From Faxitron Images[a]

	Avg Coated Ingrowth		Avg Uncoated Ingrowth			
Study Group	%	SE	%	SE	*p* Value	Sample Size, n
6 week	77.37	8.89	60.26	6.71	0.013	30
8 week	83.23	7.26	61.23	5.48		
12 week	95.43	4.57	53.62	20.20	0.318	12

[a]Sample size includes repeated measures experiments done on a total of 6 channels per animal. SE, standard error.

TABLE III
Summary of Bone Percentage Area Ingrowth Data From Histological Slides[a]

	Avg Coated Ingrowth		Avg Uncoated Ingrowth			
Study Group	%	SE	%	SE	*p* Value	Sample Size, n
6 week	32.20	5.18	11.12	2.45	0.001	30
8 week	36.27	4.23	10.90	1.99		
12 week	39.55	21.38	7.26	3.49	0.19	12

[a]Sample size includes repeated measures experiments done on a total of 6 channels per animal. SE, standard error.

Comparison of histological slide measurements and faxitron measurements exhibited equivalent percentages within acceptable error (within a 5% difference), so it was concluded that histological slides display an accurate view of bone ingrowth into the various channels. While analysis of histological slides trended towards significant differences between treatments ($p = 0.065$), faxitron images did show a clear significant difference ($p = 0.013$). It can be concluded that although bone did grow into the uncoated channels, uncoated channels in all study groups contained bone that was surrounded by a fibrous tissue sheath (Fig. 2). This suggests that area ingrowth and continuous bone apposition measurements may be a better indication of the performance of the apatite coating.

Area ingrowth

The second phase of evaluation was performed by quantifying the extent of area ingrowth into each coated and uncoated channel of each chamber. Data showed that percent area ingrowth in coated channels was significantly higher than in uncoated channels ($p = 0.001$). Since analysis of faxitron images verified that the sections taken for histology contained the plane with the greatest extent of ingrowth, it was assumed that area ingrowth was also maximal in the histology slides. SEM images that were acquired were also measured for area ingrowth, and it was found that the percentages were equivalent, within acceptable error (within a 5% difference). Therefore, histology results were again validated.

Continuous bone apposition

The third phase of evaluation was performed by quantifying the extent of bone in direct apposition to the control or experimental surfaces of the coupons forming the channel walls. Data showed that percent continuous bone apposition in coated channels was significantly higher than in uncoated channels. Previous studies have shown that there may be a correlation between direct bone apposition to a metal surface and mechanical strength of the interface: the greater the direct bone apposition, the greater the mechanical strength.[40] Based on this assumption, the coating may in fact improve the mechanical fixation, at least in the short term. However, mechanical strength tests were not done on these chambers to validate such a correlation.

Coating resorption

In this study, examination of all time periods with histology and backscattered electron imaging (BEI) appears to show resorption of the apatite coating after implantation. BEI showed that 6- and 8-week samples seemed to exhibit the stable coating only in areas where bone was in direct contact with the apatite surface. Coating was not observed in other areas (Fig. 5). Coating was also not visible in the 12-week samples, even in areas with direct bone apposition. This observation suggests that the coating may be degrading once implanted in vivo, and may be stabilized by the attachment to bone ini-

TABLE IV
Summary of Bone Percentage Area Ingrowth Data From SEM Images[a]

	Avg Coated Ingrowth		Avg Uncoated Ingrowth			
Study Group	%	SE	%	SE	*p* Value	Sample Size, n
6 week	31.71	4.25	11.71	2.55	0.001	30
8 week	33.22	3.47	12.28	2.08		
12 week	38.55	23.63	6.60	3.01	0.22	12

[a]Sample size includes repeated measures experiments done on a total of 6 channels per animal. SE, standard error.

TABLE V
Summary of Continuous Bone Apposition % Data from Histological Slides[a]

	Avg Coated Ingrowth		Avg Uncoated Ingrowth			
Study Group	%	SE	%	SE	*p* Value	Sample Size, n
6 week	28.45	8.37	4.11	1.92	0.014	30
8 week	22.12	6.84	2.75	1.57		
12 week	16.79	6.75	0	0	0.08	12

[a]Sample size includes repeated measures experiments done on a total of 6 channels per animal. SE, standard error.

tially. It may then become incorporated in the new bone and then remodeled as the bone matures. No distinction in the coating/bone interface is, therefore, observed. Certain studies have demonstrated that some calcium phosphate coatings can be site-specifically resorbed by osteoclasts.[41,42] Therefore, these coatings are not only osteoconductive, but they can also be replaced by bone during normal tissue remodeling. This may be an additional factor in initiating a better fixation of a coated implant to bone.

Temporal bone formation

Analysis of treatment versus time exhibited a general peak in bone ingrowth between 6 and 8 weeks post-surgery, with a decline in ingrowth at the 12-week time period in uncoated channels. Coated channels seemed to show a general increase in linear bone ingrowth and area bone ingrowth as time progressed. Continuous bone apposition percentages seemed to decrease with time in these coated channels. This indicates that osteoblast activity dominates for the first 8 weeks during new bone formation, with greater osteoclast activity occurring after that time period in areas surrounding non-coated implants. Implants covered with the apatite coating, however, seem to keep increasing the amount of surrounding bone matrix through 12 weeks post-implantation, with an increasing amount of osteoclast-mediated bone resorption and remodeling at the interface between implant and bone as time progresses. These results are in agreement with previous bone chamber studies.[36,37]

CONCLUSIONS

This study established the following:

1. Histology and BEI analysis demonstrated resorption of the coating 6 and 8 weeks after implantation. The coating seemed to be stabilized in the areas where bone had become apposed to the surface;
2. The linear ingrowth percentages in histology slides did not differ significantly between the two treatments in all study groups, but did show a trend in increasing ingrowth in coated

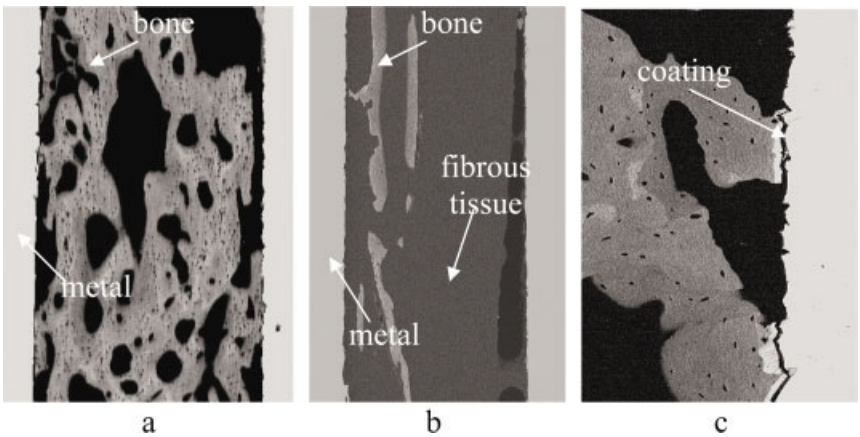

Figure 5. (a) SEM/BEI of a coated channel at 8 weeks showing greater area ingrowth and continuous bone apposition to the metallic surface. (b) SEM/BEI of an uncoated channel at 8 weeks showing greater fibrous tissue encapsulation with minimal bone area ingrowth. (c) SEM/BEI of a coated channel at 8 weeks showing stabilization of coating at bone-to-metal contact points. [Color figure can be viewed in the online issue, which is available at www.interscience.wiley.com.]

channels and a decreasing ingrowth in uncoated channels. Faxition analysis of linear ingrowth %, however, did show a significant difference between treatments;

3. Area ingrowth and apposition percentages exhibited significant increases in coated channels versus uncoated channels in all study groups ($p < 0.05$). Since linear ingrowth (via faxitron analysis), area ingrowth, and continuous bone apposition percentages were significantly higher in coated channels than in uncoated channels, this new biomimetic apatite coating may, in fact, encourage early bone ingrowth and thereby improve the fixation of an implant to bone.

References

1. Giliberti Danielle C., Anderson Kimberly A., Dee Kay C. A jet impingement investigation of osteoblastic cell adhesion. J Biomed Mater Res 2002;62:422.
2. Wright Timothy M., Goodman Stuart B. What is the clinical scope of implant wear in the hip and how has it changed since 1995? In: Wright Timothy M, Goodman Stuart B, editors. Implant wear in total joint replacement. IL: American Academy of Orthopaedic Surgeons; 2001.
3. Giddings VL, Kurtz SM, Jewett CW, et al. A small punch test technique for characterizing the elastic modulus and fracture behavior of PMMA bone cement used in total joint replacement. Biomaterials 2001;22:1875.
4. Park K.D., Kang YH., Park JB. Interfacial strength between molded UHMWPE and PMMA-MMA monomer treated UHMWPE. J Long-Term Effects Med Implant 1999;9:303.
5. DiMaio FR, et al. The science of bone cement: a historical review. Orthopaedics 2002;25:1399.
6. Abdel-Kader KR, et al. Boneloc bone cement: experience in hip arthroplasty during a 3 year period. J Arthroplasty 2001;6:811.
7. Miyaguchi M, Kobayashi A, et al. Human monocyte response to retrieved polymethylmethacrylate particles. J Biomed Mater Res 2002;62:331.
8. Amstutz H.C. Hip arthroplasty today and tomorrow. Orthopaedics 1987;10:1759.
9. Galante JO, Lemons J, et al. The biologic effects of implant materials. J Orthopaed Res 1991;9:760.
10. Delaunay C, Kapandji AI. Survival analysis of cementless grit-based titanium total hip arthroplasties. J Bone Joint Surg 2001; 83B:408.
11. Maniatopoulos C, Pillar RM, Smith DC. Threaded versus porous-surfaced designs for implant stabilization in bone-endodontic implant model. J Biomed Mater Res 1986;20:1309.
12. Linder L, Obrant K, Boibin G. Osseointegration of metallic implants. Acta Orthopaed Scand 1989;60:135.
13. Thomas KA, Cook SD. An evaluation of variables influencing implant fixation by direct bone apposition. J Biomed Mater Res 1985;19:875.
14. Van Blitterswijk CA, Bakker D, Hesseling SC, et al. Reactions of cells at implant surfaces. Biomaterials 1991;12:187.
15. Nayak NK, Mulliken B, et al. Osteolysis in cemented versus cementless acetabular components. J Arthroplasty 1996;11:135.
16. Rorabeck CHl, Bourne RB, et al. Comparative results of cemented and cementless total hip arthroplasty. Clin Orthopaed Relat Res 1996;325:330.
17. Cook SD, Thomas KA. Fatigue failure of noncemented porous-coated implants: a retrieval study. J Bone Joint Surg 1991;73B: 20.
18. Overgaard S, Lind M, et al. Improved fixation of porous-coated versus grit-blasted surface texture of hydroxyapatite-coated implants in dogs. Acta Orthopaed Scand 1997;68:337.
19. Bargar WL, Taylor JK. Hydroxyapatite coating of custom cementless femoral components. In: Geesink RGT, Manley MT, editors. Hydroxyapatite coatings in orthopaedic surgery. New York: Raven Press; 1993.
20. Capello WN, D'Antonio JA, et al. Hydroxyapatite in total hip arthroplasty: clinical results and critical issues. Clin Orthopaed Relat Res 1998;355:200.
21. Furlong RJ, Osborn JF. Fixation of hip prostheses by hydroxyapatite ceramic coatings. J Bone Joint Surg 1991;73B:741.
22. Hardy DCR, Frayssinet Pl, et al. Bonding of hydroxyapatite-coated femoral prostheses. J Bone Joint Surg 1991;73B:732.
23. Geesink RGT. Hydroxyapatite-coated total hip prostheses: two year clinical and roentgenographic results of 100 cases. Clin Orthopaed Relat Res 1990;261:39.
24. Tisdel CL, Goldberg VM, et al. The influence of a hydroxyapatite and tricalcium-phosphate coating on bone ingrowth into titanium fiber-metal implants. J Bone Joint Surg 1994;76A:159.
25. Geesink RGT, De Groot K, Klein CT. Chemical implant fixation using hydroxyl-apatite coatings. Clin Orthopaed 1987;225:147.
26. Lemons JE. Bioceramics. Is there a difference? Clin Orthopaed Relat Res 1990;261:153.
27. Lacefield WR. Hydroxyapatite coatings. Ann NY Acad Sci 1988;523:72.
28. Engh CA. Hip arthoplasty with a More prosthesis with porous coating: a five-year study. Clin Orthopaed Relat Res 1983;176: 52.
29. Ducheyne P. Bioceramics: material characteristics and in vivo behavior. J Biomed Mater Res 1987;21(SA2):219.
30. Ellies LG, Nelson DG, et al. Crystallographic changes in calcium phosphates during plasma-spraying. Biomaterials 1992; 13:313.
31. Dhert WJA, Klein CT, et al. A mechanical investigation of fluorapatite, magnesium whitlockite, and hydroxyapatite plasma-sprayed coatings in goats. J Biomed Mater Res 1991;25: 1183.
32. Bloebaum RD, Zou L, et al. Analysis of particles in acetabular components from patients with osteolysis. Clin Orthopaed Relat Res 1997;338:109.
33. Bloebaum RD, Beeks D, et al. Complications with hydroxyapatite particulate separation in total hip arthroplasty. Clin Orthopaed Relat Res 1994;298:19.
34. Li P. Bioactive ceramic coating and method. United States Patent 6, 139, 585, 31 October 2000.
35. Spivak JM, Ricci JL, Blumenthal NC, et al. A new canine model to evaluate the biological response of intramedullary bone to implant materials and surfaces. J Biomed Mater Res 1990;24: 1121.
36. Ricci JL, Alexander H, Nadkarni P, et al. Biological mechanisms of calcium sulfate replacement by bone. In: Davies JE, editor. Bone Engineering. Toronto, Canada: EM^2 Inc.; 2000
37. Li P. Biomimetic nano-apatite coating capable of promoting bone ingrowth. J Biomed Mater Res 2003;66A:79.
38. Tracy BM, Doremus RH. Direct electron microscopy studies of the bone-hydroxyapatite interface. J Biomed Mater Res 1984; 18:719.
39. Kitsuga T, Nakamura T, Yamamuro T, et al. SEM-EPMA observation of three types of apatite-containing glass ceramics implanted in bone. J Biomed Mater Res 1987;21:1255.
40. Ducheyne P, Hench LL, Kagan A, et al. Effect of hydroxyapatite impregnaton on skeletal bonding of porous coated implants. J Biomed Mater Res 1980;14:225.
41. Davies JE. Mechanisms of endosseus integration. Int J Prosthodont 1998;11:391.
42. Davies JE, Shapiro G, et al. Osteoclast resorption of calcium phosphate ceramic thin films. Cell Mater 1993;3:245.